

Phonon dispersion and lifetimes in  $\text{MgB}_2$ 

Abhay Shukla,<sup>1</sup> Matteo Calandra,<sup>1</sup> Matteo d'Astuto,<sup>2</sup> Michele Lazzeri,<sup>1</sup> Francesco Mauri,<sup>1</sup> Christophe Bellin,<sup>1</sup> Michael Kirsch,<sup>2</sup> J. Karpiński,<sup>3</sup> S.M. Kazakov,<sup>3</sup> J. Jun,<sup>3</sup> D. Daghero,<sup>4</sup> and K. Parlinski<sup>5</sup>

<sup>1</sup>Laboratoire de Minéralogie-Cristallographie, case 115, 4 Place Jussieu, 75252, Paris cedex 05, France

<sup>2</sup>European Synchrotron Radiation Facility, BP 220, F-38043 Grenoble cedex, France

<sup>3</sup>Solid State Physics Laboratory, ETH, CH-8093 Zurich, Switzerland

<sup>4</sup>INFN - Dipartimento di Fisica, Politecnico di Torino, C. Duca degli Abruzzi 24, 10129 Torino, Italy

<sup>5</sup>Institute of Nuclear Physics, ul. Radzikowskiego, 152, 31-342, Cracow, Poland.

(Dated: January 1, 2022)

We measure phonon dispersion and linewidth in a single crystal of  $\text{MgB}_2$  along the  $\Gamma$ -A,  $\Gamma$ -M and  $\Gamma$ -L directions using inelastic X-Ray scattering. We use Density Functional Theory to compute the effect of both electron-phonon coupling and anharmonicity on the linewidth, obtaining excellent agreement with experiment. Anomalous broadening of the  $E_{2g}$  phonon mode is found all along  $\Gamma$ -A. The dominant contribution to the linewidth is always the electron-phonon coupling.

PACS numbers: 63.20.Dj, 63.20.Kr, 78.70.Ck, 71.15.Mb

The discovery of 39 K superconductivity in  $\text{MgB}_2$  [1] has led to in-depth study of the material and a picture has emerged of a phonon-mediated superconductor with multiple gaps [2, 3, 4], moderate electron-phonon coupling (EPC) [3, 5, 6, 7], and anharmonicity [3, 4, 8, 9]. However no measurements exist concerning either phonon dispersion or the evolution of phonon lifetimes over the Brillouin Zone (BZ), due to the absence of large single crystals. Neutron scattering on powder samples [8, 10] has been limited to the determination of phonon density of states. Raman spectroscopy, which is restricted to the BZ center, has shown that the optical mode with  $E_{2g}$  symmetry, corresponding to in-plane distortions of the B hexagons, is strongly damped [11, 12, 13, 14].

Phonon damping can be caused by (i) EPC mediated phonon decay into electron-hole pairs [15], or (ii) phonon-phonon interaction due to anharmonicity [16]. The linewidth (the inverse of the lifetime) of a given phonon is the sum of both contributions. Direct determination of the contribution of each phonon mode to EPC [15] from the measured linewidth is only possible if the anharmonic contribution is negligible [17] and is seemingly questionable for  $\text{MgB}_2$  where many calculations [3, 4, 8] suggest strong anharmonic effects.

In this work we present the first measured phonon dispersion curves and linewidths (where possible) along three directions in the BZ,  $\Gamma$ -A,  $\Gamma$ -M and  $\Gamma$ -L. We circumvented the problem of sample size by using high resolution inelastic scattering of a focused and intense X-Ray beam at the European Synchrotron Radiation Facility (beam line ID 28), a technique [18] successfully used in single crystalline samples and in particular for the measurement of high energy optical modes [19]. To understand the mechanisms governing the measured phenomena, we calculated phonon dispersion, the contributions of EPC and anharmonicity to the linewidth and the structure factors using Density Functional Theory (DFT).

Small single crystals of  $\text{MgB}_2$ , suitable for inelastic X-

ray scattering experiments have recently become available. The crystal used in our experiment was grown at a pressure of 30–35 kbar. A mixture of Mg and B was put into a BN container in a cubic anvil device. The temperature was increased during one hour up to 1700–1800 K, kept stable for 1–3 hours and decreased during 1–2 hours. As a result plate-like  $\text{MgB}_2$  crystals were formed of which we used a sample of about  $400 \times 470 \times 40 \text{ } \mu\text{m}^3$ ; with a measured in-plane mosaicity of  $0.007^\circ$ . The beam incident on the sample was obtained from a high-resolution Silicon backscattering monochromator using the (8 8 8) reflection at an incident energy of 15.816 keV. The X-ray beam was focused onto the sample by a toroidal mirror into a spot of  $270 \times 90 \text{ } \mu\text{m}^2$  (horizontal vertical), full width at half maximum (FWHM). Slits before the sample further limited the vertical beam size to  $30 \text{ } \mu\text{m}$ . The scattered photons were analyzed in energy by five spherical silicon crystal analyzers operating at the same reflection order and mounted in pseudo Rowland circle geometry. The total energy resolution was  $6.1 \text{ meV FWHM}$ , as determined by a fit to a Lorentzian lineshape. The momentum transfer  $Q$  was selected by rotating the 7 m long analyzer arm around the sample position, in the horizontal plane, which also contained the linear x-ray polarization vector of the incident beam. The momentum resolution was set to  $0.04 \text{ } \text{\AA}^{-1}$  in the horizontal direction and  $0.07 \text{ } \text{\AA}^{-1}$  in the vertical direction. The following measurements were performed at a temperature of 300 K: i)  $Q = (1 \ 2 \ 0)$ , in almost transverse configuration along the  $\Gamma$ -A direction, i.e. with  $Q \cdot q = 0$ ,  $q = (0 \ 0 \ 0)$  being the phonon wavevector, ii)  $Q = (1 \ -1 \ 0)$ , while nearly following the  $\Gamma$ -M direction  $(0 \ 0 \ 0.05)$ . iii)  $Q = (1 \ -1 \ 2 \ 0.5 \ 2)$ , while nearly following the  $\Gamma$ -L direction  $(0 \ 1 \ 2 \ 0.04)$ . The choice of BZ points measured was dependent on a series of conditions including the need to optimize the structure factors, single ( $\Gamma$ -A) or multi-analyzer ( $\Gamma$ -M,  $\Gamma$ -L) measurement mode and spectrometer and time limitations.

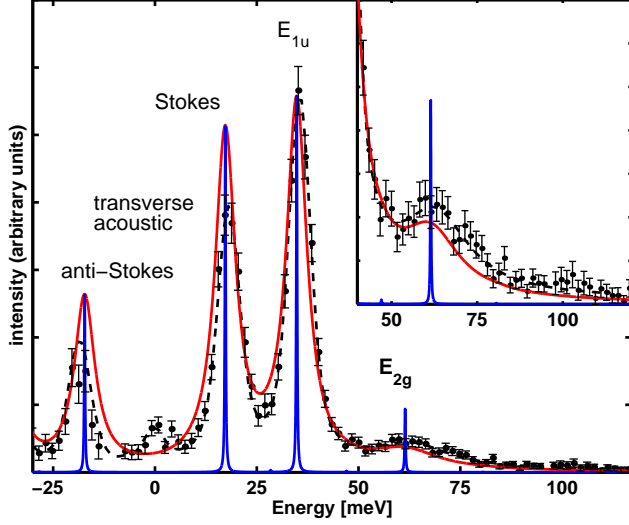


FIG. 1: (color online) Energy loss scan in almost transverse geometry measured at  $Q = (1\ 2\ 0.3)$  corresponding to  $0.6\ -A$ . The data, normalized to the incident flux, are shown with the least-squares fit (dashed line) and the ab-initio spectrum with and without broadening due to experiment and electron phonon coupling (solid lines). The broad peak corresponds to the damped  $E_{2g}$  mode and is shown in greater detail in the inset. The peak at zero is due to diffuse scattering.

In Fig. 1 we show data taken at the  $0.6\ -A$  point in the BZ. The acoustic mode as well as the lower energy optical mode ( $E_{1u}$ ) are visible as resolution-limited peaks. Most importantly, a broad peak is observed at higher energy loss, corresponding to the  $E_{2g}$  mode. We performed least square fits to sums of Lorentzian functions with FWHM corresponding to the experimental resolution for the resolution limited peaks and a free parameter for the strongly damped phonon. These yield the dispersion as well as the linewidth variation over the BZ. Despite statistical limitations (3-6 counts per minute on this peak along  $-A$ ) and tails of the peaks from the stronger, low energy phonons, the peak energy as well as the linewidth can be estimated with reasonable confidence.

Fig. 2 shows a similar energy loss scan at  $(0.97\ 2.29\ 0.54)$  close to the  $0.58A-L$  point. A strong acoustic mode is seen at 30 meV. The peak at 50 meV corresponds to the  $A_{2u}$  branch and the one at 65 meV to another acoustic branch. Finally two resolved features are seen at 85 and 97 meV. These are the two  $E_{2g}$  modes which in this region of reciprocal space are well separated from other modes. Though, given the statistics, it would be hazardous to estimate a linewidth, the comparison between the experimental and ab-initio spectra suggests that the linewidths of both the  $E_{2g}$  modes are resolution limited and so the damping is much less than that along  $-A$ . As for the measurement nearly along  $-M$ , the structure factor for the optical modes strengthens only near the

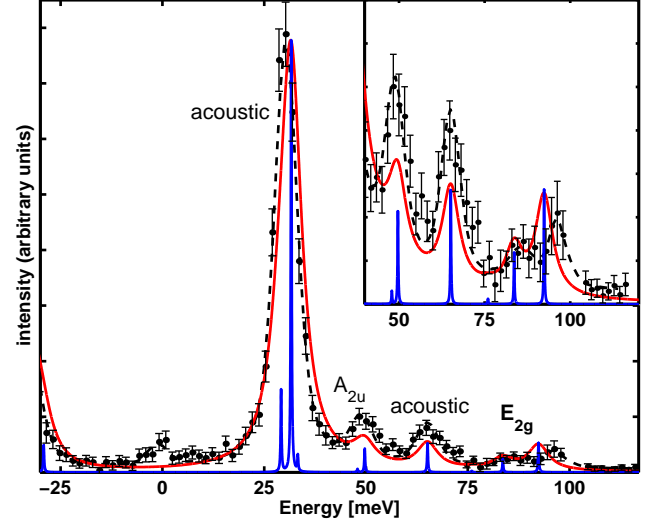


FIG. 2: (color online) Energy loss scan, measured at  $Q = (0.97\ 2.29\ 0.54)$  corresponding closely to  $0.58\ A-L$ , with the least-squares fit and the ab-initio spectrum calculated at  $0.58\ A-L$ .

zone boundary. At the point measured nearest to  $M$  ( $1.05\ 1.45\ 0$ ), not shown) the  $E_{2g}$  and  $E_{1u}$  modes are comparable in intensity but only separated by about 1 meV according to our calculation and we do measure a single peak only somewhat broader (FWHM  $\sim 10$  meV) than the experimental resolution, indicating reduced  $E_{2g}$  linewidth. The proximity of the  $E_{1u}$  mode however prevents a firm conclusion in this regard. We mention that the calculated structure factors and energies show excellent quantitative agreement with our measured data of which we have shown only two examples.

Similar analysis was done for several points along the three directions in order to experimentally determine the phonon dispersion and the linewidths. The difference in calculated phonon energies between the measured points and corresponding points exactly along  $-M$  and  $A-L$  ( $\delta_1; \delta_2 = 0$ ) is less than half a meV in all cases. We can thus compare the experimental phonon dispersion with the theoretical calculation along the high symmetry lines, as shown in the bottom panel of Fig. 3 (circles).

The measured intrinsic linewidth of the  $E_{2g}$  branch, shown in the top panel of Fig. 3, is strongly anisotropic in the BZ. Along  $-A$  it is particularly large (ranging from 20 to 28 meV), while near  $L$  and probably near  $M$  it is below the experimental resolution.

Electronic structure calculations [20] were performed using DFT in the generalized gradient approximation [21]. We used norm conserving pseudo-potentials [22]. For Mg we used non-linear core corrections [23] and we treated the 2s, 2p levels as core states. The wavefunctions were expanded in plane waves using a 35 Ry cutoff. The calculations were performed with the experimental crystal structure, namely  $a = 3.083\text{\AA}$  and  $c/a =$

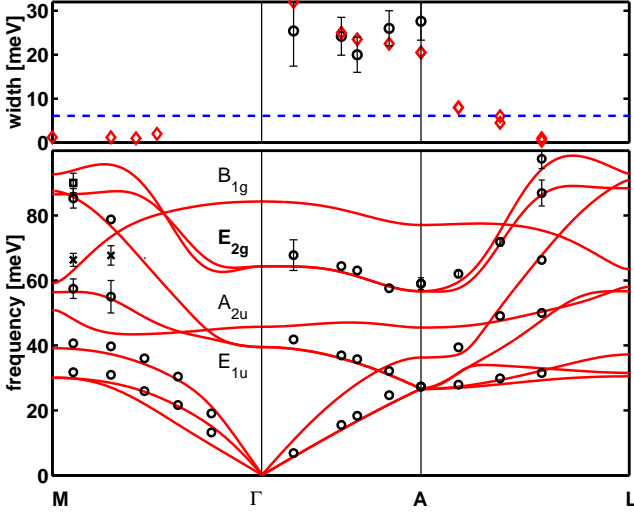


FIG. 3: (color online) Bottom : Experimental (circles) and theoretical phonon dispersion (solid line) in  $\text{MgB}_2$  along  $\Gamma$ -A and  $\Gamma$ -M and A-L. In the region near the M point, the probable detection of the  $E_{2g}$  mode is indicated with a square symbol (see text). The crosses indicate a parasite signal of unknown origin. Top: Intrinsic linewidth of the  $E_{2g}$  mode. The experimental linewidth (circles) is large along  $\Gamma$ -A and below the experimental resolution (dashed line) near L and M. The theoretical result (diamonds) for the electron-phonon coupling contribution to the linewidth is also shown. Along A-L and  $\Gamma$ -M where the  $E_{2g}$  mode is non-degenerate both theoretical values are shown, when different.  $E_{2g}$  linewidth decreases progressively from A to L and experimentally the two branches are resolved for the point nearest to L.

1:142. The harmonic phonon frequencies were computed in the linear response [24]. We used a  $16 \times 16 \times 16$  Monkhorst-Pack grid for the electronic BZ integration and first order Hermite-Gaussian smearing [25] of 0.025 Ry. The dynamical matrix at a given point of the BZ was obtained from a Fourier interpolation of the dynamical matrices computed on a  $6 \times 6 \times 4$  phonon mesh. The resulting phonon frequencies are shown in Fig. 3 and are in good agreement with a recent calculation [11]. The agreement with experiment is remarkable.

The contribution to the FWHM linewidth  $\gamma_q$  at momentum  $q$  for the  $E_{2g}$  phonon mode due to the electron-phonon interaction can be written as [15]:

$$\gamma_q = \frac{4}{N_k} \sum_{k,n,m} \frac{|\langle k+n, k+q | V | k, n \rangle|^2}{\omega_{k+n} \omega_{k+q}} \left( n_{k+n} + \frac{1}{2} \right) \left( n_{k+q} + \frac{1}{2} \right) \quad (1)$$

where the sum is extended over the BZ,  $N_k$  is the number of  $k$ -points in the sum, and  $\epsilon_{k,n}$  are the energy bands measured with respect to the Fermi level at point  $k$ . The matrix element is  $g_{k+n, k+q} = \langle k+n, k+q | V | k, n \rangle$ , where  $u_q$  is the amplitude of the displacement of the phonon of wavevector  $q$ ,  $\omega_q$  is the phonon frequency and  $V$  is the Kohn-Sham potential.

In the calculations we used  $N_k = 30^3$  inequivalent  $k$ -points and, in Eqs. (1) and (3), we substituted the functions with Gaussians. The electron phonon coupling  $\gamma_q$  is obtained from the linewidth [15] as:

$$\gamma_q = \frac{\gamma_q}{2 N(0) \omega_q^2}; \quad (2)$$

$N(0) = 0.354$  states/(MeV spin) being the density of states at the Fermi level.

The second contribution to the linewidth is given by the anharmonicity in the crystal potential. At lowest order for the  $E_{2g}$  mode of a zone center phonon the FWHM linewidth is [16, 26, 27]:

$$\gamma_q = \frac{\hbar}{8 N_q \omega_q} \left[ \frac{\partial^3 E}{\partial u_0 \partial u_q \partial u_q} \right]^2 \frac{I_q^D}{\omega_q} + \frac{I_q^A}{\omega_q} \quad (3)$$

$E$  being the total energy,  $n_q$  the Bose occupation for mode at wavevector  $q$ ,  $I_q^D = (n_q + n_q + 1) \omega_q$  describes the decay in the two phonons and  $I_q^A = 2(n_q + 1) \omega_q$  describes the  $E_{2g}$ -phonon absorption and the  $E_{2g}$ -phonon emission.

We computed the anharmonic linewidth at the high-symmetry points  $\Gamma$ , A, M. For the calculation at A we considered a  $1 \times 1 \times 2$  supercell with 6 atoms, while for the M point we used a  $2 \times 2 \times 1$  cell with 12 atoms. The third order matrices were evaluated using linear response theory and the  $2n+1$  theorem for metals [28]. The anharmonic contribution was evaluated at 0K and 300K.

At  $\Gamma$  the anharmonic linewidth is largest for the  $E_{2g}$  mode and equal to 0.16 meV at  $T = 0K$  and 1.21 meV at  $T = 300K$ . Both the values are negligible if compared with the experimental Raman linewidth of roughly 40 meV [13], suggesting that the main source of broadening is the electron-phonon interaction.

The results of the calculation of the two contributions to the linewidth at A and M are shown in Table I. At the A point the linewidth of the  $E_{2g}$  mode due to electron-phonon scattering is very large while the anharmonic contribution is more than an order of magnitude smaller. For sizable values of the EPC and at low temperature the anharmonicity is negligible showing that a measurement of the linewidth at  $q$  for the  $E_{2g}$  mode is essentially equivalent to determining  $\gamma_q$ . This is unexpected since earlier theoretical work [3, 4, 8] estimates anharmonicity to be important for a different but related quantity, the frequency shift.

Since the anharmonic contribution is negligible at  $\Gamma$ , A, M, and computationally demanding, we only evaluated the EPC linewidth for the other points along the three directions. Using the calculated phonon frequencies, displacements and linewidths we compute the structure factors for one phonon processes using the X-ray form factors, obtaining good agreement with experiment as shown in Figs. 1,2. In the top panel of Fig. 3 we show

M				A			
0	300	0	300	0	300	0	300
0.00	0.12	0.00	0.00	0.00	0.17	0.00	0.00
0.00	0.15	0.01	0.01	0.00	0.17	0.00	0.00
0.02	0.12	0.06	0.02	0.00	0.63	0.08	0.05
0.12	0.48	1.13	0.20	0.00	0.63	0.08	0.05
0.06	0.25	0.00	0.00	0.02	0.22	0.84	0.28
0.07	0.33	2.34	0.30	0.02	0.20	0.08	0.02
0.26	0.42	1.06	0.06	0.10	2.13	20.35	2.83
0.45	0.69	1.21	0.07	0.10	2.13	20.35	2.83
0.47	0.72	0.08	0.00	0.13	0.23	0.05	0.00

TABLE I: Calculated linewidths (meV) due to anharmonicity at 0K (0), 300K (300) and electron-phonon interaction at M and A for all modes. Phonon frequencies increase from top to bottom.  $\lambda$  is the electron-phonon coupling.  $E_{2g}$  modes in boldface.

q	0.2 -A	0.5 -A	0.6 -A	0.8 -A	1.0 -A
$q_{\text{expt}}$	2.5 1.1	2.6 0.6	2.3 0.5	3.6 0.7	3.6 0.8
$q_{\text{theo}}$	3.32	2.80	2.77	3.12	2.83

TABLE II: Experimental and theoretical  $q$  of each of the two degenerate  $E_{2g}$  modes along -A.

the theoretical results for the  $E_{2g}$  branch. The result is consistent with the experimental value wherever the  $E_{2g}$  branch is clearly visible namely along -A and near the L point. Finally, the anharmonicity being negligible, we used Eq. (2) to extract  $q$  of the  $E_{2g}$  mode along -A using the measured linewidths and frequencies together with the calculated electronic density of states. In Table II the experimental values are compared with the theoretical predictions. The anomalously large EPC along -A is due to the nesting factor of the B bonding  $p_{xy}$  Fermi surfaces, which are concentric cylinders centered on -A [5, 6]. The  $E_{2g}$  modes, which modify the B-B distances, are the only ones with a sizeable matrix element,  $g_{k_n, k_n + q_m}$ , between electrons on these surfaces.

In conclusion, we have measured phonon dispersion and linewidths in a sub-mm sized  $\text{MgB}_2$  crystal with inelastic X-ray scattering confirming the power and versatility of this technique. Both acoustic and optical modes are detected and we find that the  $E_{2g}$  mode is anomalously broadened along -A but that this broadening is not generalized over the Brillouin Zone. Our Density Functional Theory calculations of the dispersion and linewidth are in excellent agreement with experiment. They show that the dominant contribution to the broadening for all modes is the electron-phonon coupling, the anharmonic contribution being much smaller. Thus phonon linewidth in  $\text{MgB}_2$  is a direct measure of electron-phonon coupling and could, with the availability of larger

samples, be measured for all modes over the whole Brillouin zone so as to extract the anisotropic Eliashberg coupling function.

We acknowledge illuminating discussions with R. S. Gonnelli, P. Giannozzi, M. Xu, and F. Sette. The calculations were performed at the IDRIS supercomputing center. M.C. was supported by a Marie Curie Fellowship of the European Commission, contract No. IHP-HPMF-CT-2001-01185.

- [1] J. Nagamatsu et al, Nature (London) 410, 63 (2001).
- [2] S.V. Shulga et al cond-mat/0103154.
- [3] A.Y. Liu, I.I. Mazin and J.Kortus, Phys. Rev. Lett. 87, 087005 (2001).
- [4] H.J. Choi et al, Nature (London) 418, 758 (2002), H. J. Choi et al, Phys. Rev. B 66, 020513 (2002)
- [5] J.M. An and W.E. Pickett, Phys. Rev. Lett. 86, 4366 (2001), J.M. An et al cond-mat/0207542
- [6] J.Kortus et al, Phys. Rev. Lett., 86, 4656 (2001).
- [7] Y. Kong et al Phys. Rev. B, 64, 020501(R) (2001).
- [8] T. Yildirim et al Phys. Rev. Lett. 87, 37001 (2001).
- [9] L. Boeriet al, Phys. Rev. B 65, 214501 (2002)
- [10] R. Osborn et al Phys. Rev. Lett. 87, 17005 (2001)
- [11] K.P. Bohnen, R. Heid and B. Renker, Phys. Rev. Lett. 86 5771 (2001).
- [12] A.F. Goncharov et al Phys. Rev. B 64, 100509 (2001)
- [13] P. Postorino et al Phys. Rev. B 65 020507(R) (2001)
- [14] J.Hlinka et al Phys. Rev. B 64, 140503(R) (2001)
- [15] P.B. Allen, Phys. Rev. B 6, 2577 (1972), P.B. Allen and R. Silbergliitt, Phys. Rev. B 9, 4733 (1974).
- [16] J. Menendez and M. Cardona, Phys. Rev. B 29 2051 (1984)
- [17] G. Grimvall, The electron-phonon interaction in metals, (North Holland, Amsterdam, 1981) p. 201.
- [18] T. Ruf et al Phys. Rev. Lett. 86, 906 (2001)
- [19] M.D'Astuto et al Phys. Rev. Lett. 88, 167002 (2002).
- [20] S. Baroni, et al Rev. Mod. Phys. 73, 515-562 (2001).
- [21] J.P. Perdew, K. Burke, M. Ernzerhof, Phys. Rev. Lett. 77, 3865 (1996)
- [22] N. Troullier and J.L. Martins, Phys. Rev. B 43, 1993 (1991).
- [23] S.G. Louie, S. Froyen, and M.L. Cohen, Phys. Rev. B 26, 1738 (1982)
- [24] P. Giannozzi et al, Phys. Rev. B 43, 7231 (1991)
- [25] S. de Gironcoli, Phys. Rev. B 51, 6773 (1995)
- [26] A. Debernardi, S. Baroni and E. Molinari Phys. Rev. Lett. 75, 1819 (1995)
- [27] G. Lang et al Phys. Rev. B 59, 6182 (1999)
- [28] M. Lazzeri and S. de Gironcoli Phys. Rev. B 65, 245402 (2002). For the electronic BZ integration we used a  $14 \times 14 \times 8, 14 \times 14 \times 4, 7 \times 7 \times 8$  mesh for the calculation at  $\Gamma, A, M$ , respectively. The third order derivative of the total energy were computed with a  $4 \times 4 \times 2, 4 \times 4 \times 1$  and  $2 \times 2 \times 2$  mesh of q points for  $\Gamma, A, M$  respectively and Fourier interpolated at the points q required for the BZ summation in Eq. (3). We performed the q BZ summation using a  $20^3$  grid of inequivalent points.